Magnetic domain coupling study in single-crystalline Fe/CoO bilayers

2009 J. Phys.: Condens. Matter 21 185004

(http://iopscience.iop.org/0953-8984/21/18/185004)

J. Phys.: Condens. Matter **21** (2009) 185004 (6pp) doi:10.1088/0953-8984/21/18/185004

Magnetic domain coupling study in single-crystalline Fe/CoO bilayers

J Miguel[1], R Abrudan[1,2,3], M Bernien[1], M Piantek[1], C Tieg[2,4], J Kirschner[2] and W Kuch[1]

[1] Institut für Experimentalphysik, Freie Universität Berlin, Arnimallee 14, D-14195 Berlin, Germany
[2] Max-Planck-Institut für Mikrostrukturphysik, Weinberg 2, D-06120 Halle, Germany

E-mail: radu.abrudan@bessy.de

Received 13 October 2008, in final form 3 February 2009
Published 11 March 2009
Online at stacks.iop.org/JPhysCM/21/185004

Abstract

We report on a study of the magnetic domain coupling in epitaxial wedge-shaped Fe layers deposited onto CoO/Ag(001). By using photoelectron emission microscopy (PEEM) in combination with x-ray magnetic circular and linear dichroism (XMCD, XMLD), we imaged the ferromagnetic and antiferromagnetic domains present in the Fe and CoO layers, respectively, below the CoO magnetic ordering temperature. The uncompensated Co spins at the Fe/CoO interface were revealed by XMCD–PEEM and were found to be coupled parallel to the magnetization of the Fe layer. An increase of the CoO XMLD contrast is visible for Fe thicknesses below 2 ML, where the Fe layer lacks magnetic long-range order.

(Some figures in this article are in colour only in the electronic version)

Exchange bias phenomena result from coupling ferromagnetic (FM) and antiferromagnetic (AFM) systems, and are characterized by a shift of the hysteresis loop along the field axis—known as the exchange bias field—and an increase of the coercive fields [1, 2]. This effect is based on the unidirectional character of the magnetic coupling at the FM/AFM interface, breaking the time-reversal symmetry of the interaction between the external field and the spin magnetic dipole. The detailed structural and magnetic characteristics of the interface play a key role in sizing the shift and width of the hysteresis loop, but irreversible processes like pinning and winding of AFM domain walls [3, 4] may lead to a history-dependent magnetic reversal behavior of the FM/AFM system [5]. Reciprocally, properties of the AFM layer such as the magnetic ordering temperature may be affected by the so-called proximity effects [6–8], while global changes like different magnetization or spin directions for the FM and AFM layers have been observed [9]. Despite the encouraging use of exchange-biased multilayered thin films in many technologically relevant devices and theoretical efforts over the last few decades [10–13], models that fully explain the myriad of related aspects have not yet been established. Many variables have been identified as possible ingredients of the exchange bias effect: roughness, strain effects between layers [14], spin rotation of the AFM near the interface [4] or layer thicknesses [15].

Aiming at simplifying the study of the exchange bias effect, single-crystalline layers appear as excellent model systems: the low density of structural defects and the absence of grain boundaries facilitate the study of FM/AFM systems. In a previous study we used x-ray magnetic circular and linear dichroic (XMCD and XMLD) spectroscopies to study epitaxially grown Fe/CoO/Ag(001) bilayers [16]. By exploiting the element, chemical and magnetic sensitivities of XMCD [17] and XMLD [18], we determined that the Co spin axis is collinear with the Fe magnetization direction along the ⟨110⟩ substrate crystallographic directions, which was later supported by comparison to atomic multiplet calculations [19]. The interfacial chemical and magnetic properties were also investigated in detail: we found an FeO layer of 0.3 ML (monolayers), and an amount of uncompensated FM Co spins of 1.1 ML.

In this paper we focus on the magnetic domain structure of wedge-shaped Fe layers on continuous CoO thin films by combining photoelectron emission microscopy (PEEM) with

[3] Present address: Institut für Experimentalphysik 4, Ruhr-Universität Bochum, D-44780 Bochum, Germany.
[4] Present address: European Synchrotron Radiation Facility, BP 220, F-38043 Grenoble, France.

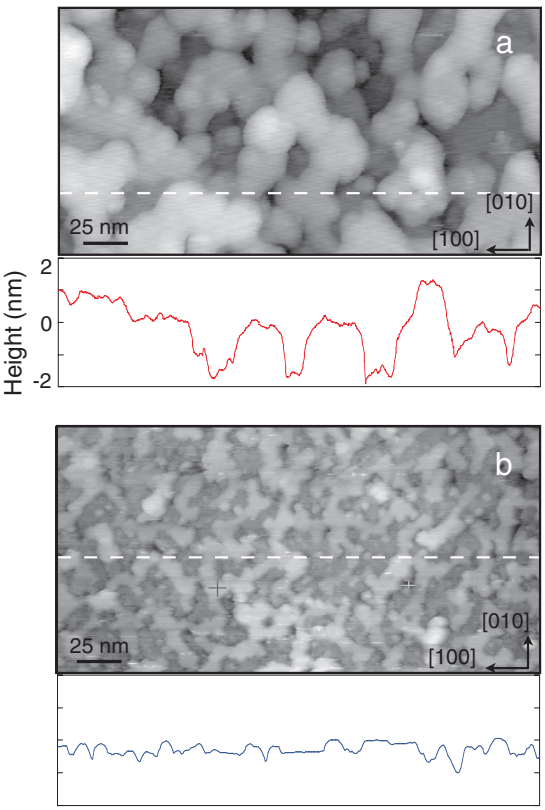

Figure 1. (Color online) STM images of the 8 ML CoO surface before (a) and after (b) annealing under an oxygen atmosphere. Bottom panels show the CoO height profile obtained at the corresponding dashed lines (typical values for tip-to-sample bias voltage and tunneling current were $V_{\text{bias}} = -2.7$ V and $I = 0.3$ nA).

XMCD and XMLD [20]. We are able to image the FM Fe domains, the AFM CoO domains and the uncompensated Co spins at the FM/AFM interface, finding a perfect overlap of the FM Fe and AFM CoO domains at low temperatures. On the verges of the Fe wedge, we observe how the CoO XMLD contrast is affected by the adjacent ultrathin Fe layer.

Prior to the bilayer preparation, the Ag(001) substrate was treated by repeated Ar^+ sputtering (750 eV) and annealing (750 K) cycles, ensuring a clean and flat surface. A continuous 8 ML thick CoO layer was deposited by electron-beam evaporation of Co onto the Ag(001) substrate at $T = 450$ K under oxygen atmosphere ($P = 1.3 \times 10^{-6}$ mbar), as described in [16]. The increased temperature avoids the creation of precursors of other oxidic phases. Further annealing of the CoO layer greatly improves the surface quality. Figure 1 shows scanning tunneling microscopy (STM) images taken before (panel (a)) and after (b) annealing up to 700 K in oxygen ambience for 30 min, where the surface topography was studied using the constant-current STM mode. Despite the insulating character of the CoO layer, its very small thickness allowed the STM measurements. It is evident how the process of annealing in oxygen atmosphere transforms the somewhat large islands seen in the as-grown layer into a much finer landscape, reducing the rms value of the CoO surface roughness of the imaged areas from 15.8 to 2.6 Å, as seen in the line profiles displayed below each image. This surface roughness is smaller than the thickness of one CoO monolayer, proving that we have a very flat FM/AFM interface. At the same time, it supports the 1.1 ML CoO of uncompensated FM Co atoms found at the interface [16].

The Fe wedge was subsequently prepared by masking the CoO/Ag(001) film with a 0.5×2 mm^2 rectangular aperture and rocking the sample holder around the axis parallel to the long side of the aperture ([010] substrate crystallographic axis) up to $\pm 15°$ at a rate of $2°$ s^{-1}, while a maximum of 5 ML Fe was evaporated onto the non-shadowed region, leading to a plateau of the same thickness [21, 22]. Figure 3(e) shows a sketch of the Fe layer, which comprises a plateau of up to 8 ML Fe and a wedge on each side of it.

The magnetic microscopy measurements were performed at the UE56/2-PGM2 beamline of BESSY. We used this monochromator and plane grating mirror beamline to produce linear and circular polarized photons with an energy resolution at the Fe and Co $L_{2,3}$ absorption edges of about 100 meV and a degree of polarization of 80%. XMCD (XMLD)–PEEM was used for layer-resolved imaging of the FM (AFM) layers [4]. Details of the experimental set-up and the instrument (*Focus* IS-PEEM) can be found in [23]. A custom-made modification allowed us to cool the sample down to ∼170 K while maintaining the rotational degree of freedom around the surface normal. The microscope parameters were set to obtain a field of view of 80 μm and a lateral resolution of about 400 nm.

The XMCD–PEEM images presented here are calculated as the asymmetry of the images taken with left- and right-circularly polarized light at the energy of maximum XMCD (see figure 2(a)). XMLD contrast [24] was obtained by exploiting the sign reversal of the Co XMLD signal at $E =$ 777.0 and 777.8 eV for the same linear s polarization (with the electric field vector **E** of the incident light in the sample plane) of the incoming beam, as shown in figure 2(b). The gray scales were adjusted to span an image contrast from white to black of $\pm 19\%$, $\pm 4\%$ and $\pm 6\%$ for the Fe XMCD–, Co XMCD– and CoO XMLD–PEEM images, respectively. Where Fe thicknesses are indicated, they are obtained from the intensity profile of the ratio between two images of the same area with the L_3 peak energy ($E = 706.8$ eV) and the L_3 pre-edge energy ($E = 700$ eV).

Figure 2(c) shows the domain pattern of the Fe layer at room temperature in the layer plateau (8 ML Fe thickness). Areas with four different gray levels are visible and their magnetization directions can be obtained by taking into account the projection of the **k** vector of the incoming light on the surface. These four directions are the magnetic easy directions of the Fe layer and coincide with the ⟨110⟩ crystallographic directions of the Ag(001) substrate. Domains as large as tens of microns cover most of the imaged area, coexisting with smaller domains of a few microns in size.

When the sample is cooled down to $T \approx 170$ K, below the CoO magnetic ordering temperature $T_{\text{AFM}} = 293$ K, the Fe XMCD–PEEM domain pattern remains unchanged (panel (d)). The CoO XMLD–PEEM image (panel (f)) shows only two levels of gray contrast. Interestingly, the black–white Fe domains coincide with the bright CoO areas, while the gray Fe areas are seen as dark contrast domains in the CoO

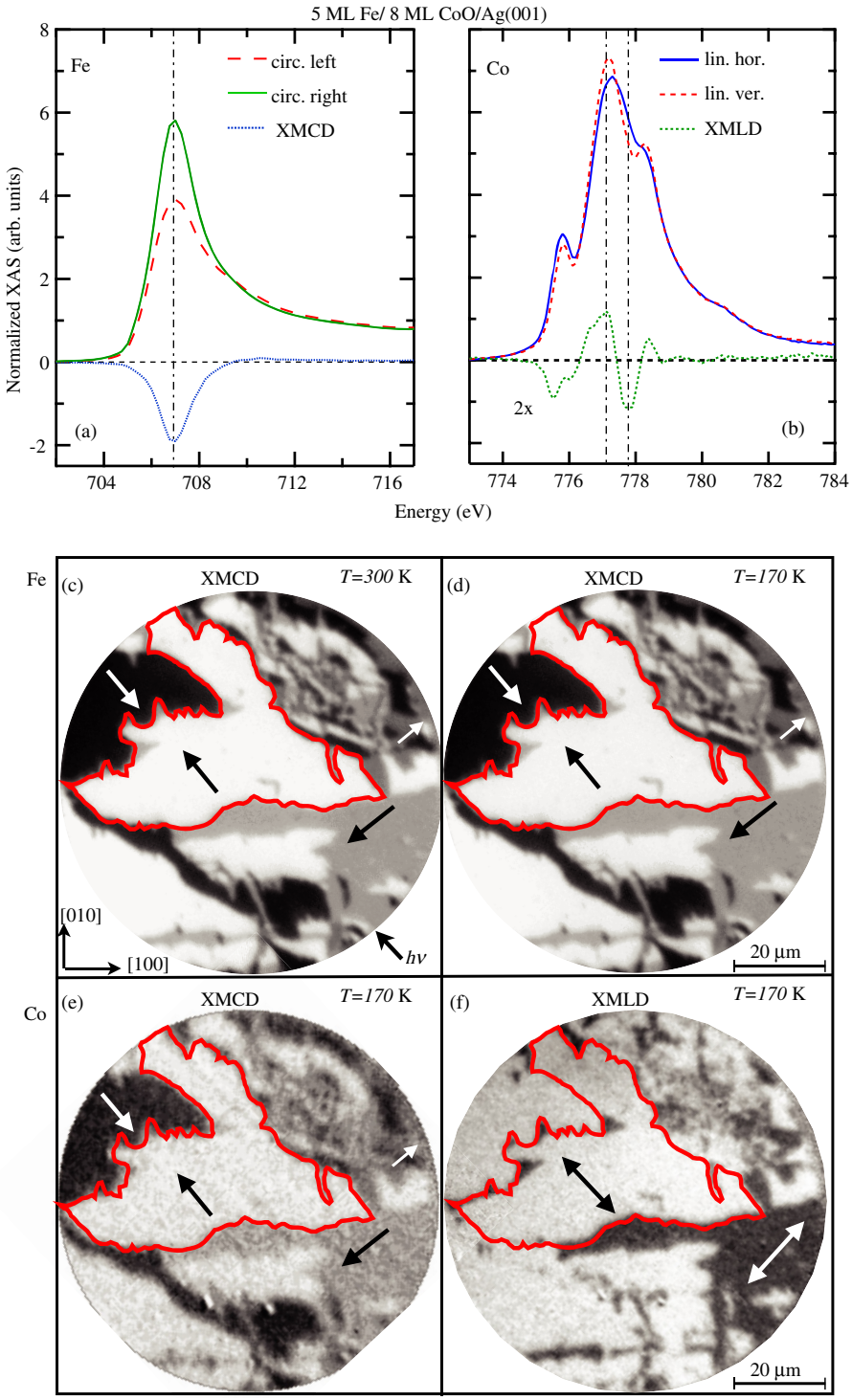

Figure 2. (Color online) The contrast mechanisms used for XMCD– and XMLD–PEEM are presented in panels (a) and (b), which show the Fe L_3 XMCD signal and Co L_3 XMLD signal, respectively. (c) XMCD–PEEM magnetic domain images of 5 ML Fe at room temperature and (d) at low temperature. (e) Magnetic domain image originating from uncompensated Co moments at the interface as seen by Co L_3 XMCD–PEEM and (f) AFM domains of the 8 ML CoO layer (Co L_3 XMLD–PEEM), both at low temperature. The red lines are guides to the eye to follow the overlap of Fe and CoO domain walls.

layer, as can be seen by following the red lines in panels (c)–(f). This overlap of domain walls is evident even in the finest domains within our lateral resolution, indicating that the Fe layer imprints its domain pattern in the CoO layer as the latter becomes magnetically ordered. Although the CoO spin axis cannot be unambiguously determined from PEEM measurements alone [25], we make use of the information obtained from continuous films, where a parallel coupling between the Fe magnetization and the Co spin axes was derived [16], so that we can infer the directions marked by arrows in figure 2(f) as the laterally resolved Co spin axes. By using now circularly polarized light at the Co L_3 edge,

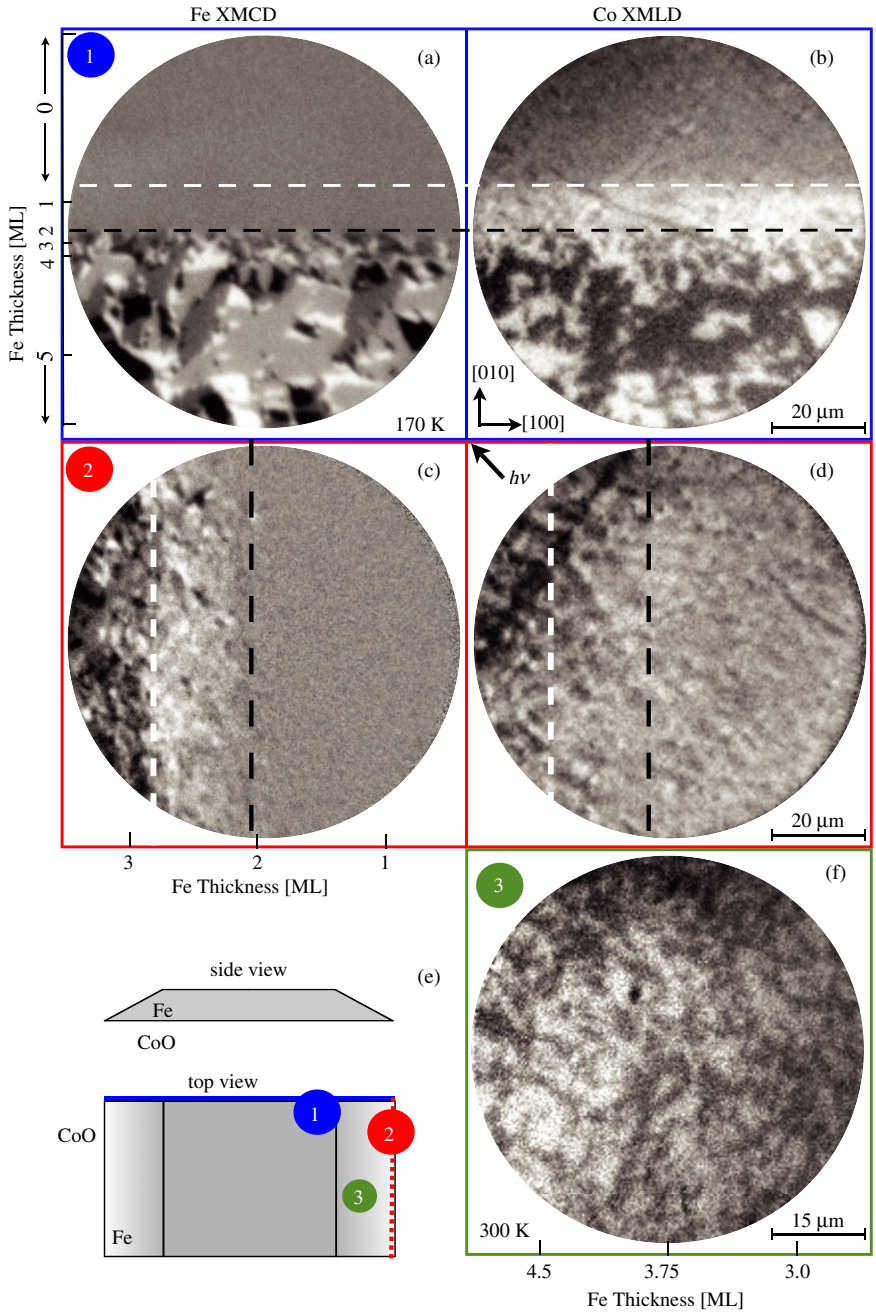

Figure 3. (Color online) According to the regions signaled in the sketch of the wedge (e), FM Fe and AFM CoO domains at the sharp (region 1, panels (a) and (b)) and broad (region 2, panels (c) and (d)) sides of the wedge, as seen by XMCD– and XMLD–PEEM at 170 K, respectively. Panel (f) shows a Co XMLD–PEEM image taken at region 3 after warming the sample back to 300 K. Arrows indicate the crystallographic directions of the substrate and dashed lines are discussed in the text.

we are also able to image the uncompensated Co spins at the interface (panel (e)), which exist within the first 1.1 ML of CoO at the interface [16]. This very small thickness results in the somehow lower contrast when compared to the Fe image. Nevertheless, the same four gray levels as for the Fe layer can be clearly observed, proving the parallel coupling between the Fe magnetization and the uncompensated Co spins. This coupling was also observed at room temperature (data not shown) and is similar to the one found on Co/FeMn [26]. Thus we conclude that the Fe layer, in this thickness range, has a strong influence on the domain pattern of the bilayer system.

In figure 3 we show the influence of the Fe layer thickness on the AFM domains of the CoO layer by imaging the two verges of the Fe wedge (indicated as regions 1 and 2 in figure 3(e)). Ultrathin Fe/Ag(001) layers display a very rich behavior in their magnetic properties, including changes in the orientation of the magnetic easy axis within the sample plane [27] and in-plane to out-of-plane spin reorientation transitions (SRT) [28] for layers thinner than ∼4 ML at 125 K. Below ∼2 ML, the FM long-range order of Fe is lost at about 300 K [29]. These effects are very sensitive to the interfacial Fe/Ag(001) properties [30] and should be

carefully considered in a comparison with the Fe/CoO/Ag(001) system.

In the case of the sharp edge (figures 3(a) and (b)), the Fe domain size decreases for smaller thickness and the Fe XMCD contrast disappears at $t_{\mathrm{Fe}}^{\mathrm{FM}} \sim 2$ ML (indicated by black dashed lines in panels ((a) and (b))), in very good agreement with literature values for the thickness of Fe/Ag(001) layers at the onset of the magnetization. Once again a perfect overlap between the Fe and CoO magnetic domain walls is seen, even at the smallest Fe domains beyond 3 ML. This is also a consequence of the interfacial flatness as shown by the STM data. In the bare CoO areas (above the white dashed lines), we succeeded in imaging the Co XMLD contrast, which shows AFM domains with typical sizes of a few microns in a rather flat contrast landscape when compared to the Fe-covered regions. In the range of 0.2 ML$<t_{\mathrm{Fe}}<$2 ML, when the Fe layer does not show any long-range magnetic order, the Co XMLD contrast seems to be perturbed by the presence of the remaining Fe layer, leading to a bright stripe in the Co image. This enhanced linear dichroic contrast, which cannot be caused by the magnetism of the Fe layer, may be explained by a change in the CoO crystallographic structure when in contact with oxidized Fe, either by oxygen donation at the Fe/CoO interface or from incipient degradation of the top Fe monolayer. The crystallographic strain in the CoO layer would result in structural linear dichroism [14, 16].

A deeper insight into these effects can be gained at the broader side of the Fe wedge (region 2). Figure 3 shows in panels (c) and (d) Fe XMCD– and Co XMLD–PEEM images, respectively, measured at 170 K. For thinner Fe regions the magnetic domains decrease both in contrast and size down to $\sim$1 μm, until the critical thickness for Fe FM order $t_{\mathrm{Fe}}^{\mathrm{FM}} \sim$ 2.1 ML (marked with black dashed lines). Surprisingly, the Fe domain distribution is not homogeneous: two regions can be observed on both sides of the white dashed line: for $t_{\mathrm{Fe}} >$ 2.8 ML, four gray levels can be seen, whereas for 2.8 ML $> t_{\mathrm{Fe}} >$ 2.1 ML, the Fe magnetic domains display predominantly a white contrast. It should be noted that the same behavior was systematically observed in other wedges and also at room temperature. This effect can be tentatively attributed to a change in the Fe magnetic easy axis from in-plane to out-of-plane when going to smaller thicknesses, in accordance with the SRT effect observed in Fe/Ag(001) layers [27–29]. Albeit the Fe/Ag(001) system is not identical to Fe/CoO/Ag(001), the relevant factors for the SRT can be assumed in the latter one: the Fe/CoO interfacial roughness as seen by STM is not larger than the typical Fe/Ag roughness and the lattice mismatch in the Fe/8 ML CoO interface is the same as in Fe/Ag(001), so that there is no additional induced anisotropy. However, the influence from tiny magnetic stray fields that would be sufficient to align such ultrathin Fe films cannot be ruled out. The absence of the same contrast in the sharp edge (figure 3(c)) can be explained by the rapidly diminishing Fe thickness.

Regarding the CoO XMLD–PEEM image (figure 3(d)), we observe that it is dominated by a brighter gray level superimposed to a certain corrugation, in agreement with the results in region 1 (except for a straight defect of the substrate running along the top left corner). For $t_{\mathrm{Fe}} >$ 2.1 ML (on the left side of the black line) small domains are seen to overlap with the Fe FM domains in the same manner as for thicker Fe areas. However, these domains continue to exist for Fe thicknesses smaller than $t_{\mathrm{Fe}}^{\mathrm{FM}}$ and are distinctively larger than the typical sizes observed in the bare CoO XMLD–PEEM image shown in the top part of figure 3(b). Furthermore, no difference is observed in the Co XMLD–PEEM image across $t_{\mathrm{Fe}} =$ 2.8 ML.

Finally, we show in figure 3(f) a Co XMLD–PEEM image taken in region 3 after the sample was brought back from 170 K to room temperature. The lower contrast as compared to the XMLD image at low temperature can be understood as being due both to the lower degree of magnetic order and to the smaller effective CoO thickness, now that the topmost monolayer is mainly ferromagnetically coupled to the Fe layer. The reduced CoO thickness would usually result in a lower AFM ordering temperature. However, the CoO domain pattern can still be distinguished at 300 K, indicating that the CoO AFM ordering temperature has increased after the cooling down/warming up magnetic history. This can be attributed to a stronger exchange anisotropy at the Fe/CoO interface once the FM/AFM coupling has been established, causing a larger and opposite change in the CoO ordering temperature.

In summary, we present an XMCD– and XMLD–PEEM study of the magnetic domain structures of the ferro/antiferromagnetic interface of ultrathin single-crystalline Fe/CoO bilayers epitaxially deposited on Ag(001). At ambient temperature, the wedge-shaped Fe layer shows magnetic domains with their magnetization aligned along the four easy $\langle 110 \rangle$ axes, and the domains decrease in size for smaller Fe thicknesses. The Fe thickness at the onset of FM order is about 2.1 ML, similar to literature values for Fe/Ag(001) layers.

Upon cooling the sample down to 170 K, the CoO layer becomes antiferromagnetically ordered, showing antiferromagnetic domains with spin axes parallel to the Fe magnetization in the plateau region, in agreement with previous spectroscopic results from the same system. By using XMCD–PEEM at the Co L_3 edge, we were able to image FM domains originating from uncompensated Co spins at the interface, proving the parallel coupling to the Fe magnetization.

For smaller Fe coverages, a perfect overlap between FM and AFM domains is found at the whole range of Fe domain sizes. At Fe regions thinner than 2 ML, the CoO domain pattern shows different linear dichroic contrast as compared to the one of the bare CoO. This can be explained by the different crystallographic structure of the CoO after donating oxygen atoms to the adjacent Fe monolayer. Furthermore a change in the AFM ordering temperature is observed after warming the Fe/CoO bilayer up to room temperature. This study reveals the microscopic character of the thickness-dependent effect of the Fe layer on the magnetic order of the CoO and has relevant implications in the understanding of the coupling between ultrathin ferro/antiferromagnetic systems.

Acknowledgments

B Zada and W Mahler are acknowledged for their technical support during the measurements. This work was supported by the DFG by grant no. KU 1115/7.

References

[1] Meiklejohn W H and Bean C P 1956 *Phys. Rev.* **102** 1413
[2] Meiklejohn W H and Bean C P 1957 *Phys. Rev.* **105** 904
[3] Nogués J and Schuller I K 1999 *J. Magn. Magn. Mater.* **192** 203
[4] Nolting F *et al* 2000 *Nature* **405** 767
[5] Hoffmann A 2004 *Phys. Rev. Lett.* **93** 097203
[6] van der Zaag P J, Ijiri Y, Borchers J A, Feiner L F, Wolf R M, Gaines J M, Erwin R W and Verheijen M A 2000 *Phys. Rev. Lett.* **84** 6102
[7] Jensen P J, Dreyssé H and Kiwi M 2005 *Eur. Phys. J.* B **46** 541
[8] Lenz K, Zander S and Kuch W 2007 *Phys. Rev. Lett.* **98** 237201
[9] Ohldag H, Scholl A, Nolting F, Anders S, Hillebrecht F U and Stöhr J 2001 *Phys. Rev. Lett.* **86** 2878
[10] Kouvel J S, Graham C D and Jacobs I S 1959 *J. Phys. Radium* **20** 198
[11] Kouvel J S and Graham J C D 1959 *J. Appl. Phys.* **30** S312
[12] Malozemoff A P 1987 *Phys. Rev.* B **35** 3679
[13] Koon N C 1997 *Phys. Rev. Lett.* **78** 4865
[14] Csiszar S I, Haverkort M W, Hu Z, Tanaka A, Hsieh H H, Lin H-J, Chen C T, Hibma T and Tjeng L H 2005 *Phys. Rev. Lett.* **95** 187205
[15] Kuch W, Chelaru L I, Fukumoto K, Porrati F, Offi F, Kotsugi M and Kirschner J 2003 *Phys. Rev.* B **67** 214403
[16] Abrudan R, Miguel J, Bernien M, Tieg C, Piantek M, Kirschner J and Kuch W 2008 *Phys. Rev.* B **77** 014411
[17] Stöhr J 1999 *J. Magn. Magn. Mater.* **200** 470
[18] van der Laan G 1999 *Phys. Rev. Lett.* **82** 640
[19] van der Laan G, Arenholz E, Chopdekar R V and Suzuki Y 2008 *Phys. Rev.* B **77** 064407
[20] Stöhr J, Wu Y, Hermsmeier B D, Samant M G, Harp G R, Koranda S, Dunham D and Tonner B P 1993 *Science* **259** 658
[21] Kuch W, Gilles J, Offi F, Kang S S, Imada S, Suga S and Kirschner J 2000 *J. Electron Spectrosc. Relat. Phenom.* **109** 249
[22] Abrudan R 2007 *PhD Thesis* Freie Universität Berlin
[23] Kuch W, Chelaru L I, Offi F, Kotsugi M and Kirschner J 2002 *J. Vac. Sci. Technol.* B **20** 2543
[24] Scholl A *et al* 2000 *Science* **287** 1014
[25] Lüning J, Nolting F, Scholl A, Ohldag H, Seo J W, Fompeyrine J, Locquet J-P and Stöhr J 2003 *Phys. Rev.* B **67** 214433
[26] Offi F, Kuch W, Chelaru L I, Fukumoto K, Kotsugi M and Kirschner J 2003 *Phys. Rev.* B **67** 094419
[27] Ballentine C A, Fink R L, Araya-Pochet J and Erskine J L 1989 *Appl. Phys.* A **49** 459
[28] Pappas D P, Brundle C R and Hopster H 1992 *Phys. Rev.* B **45** 8169
[29] Qiu Z Q, Pearson J and Bader S D 1993 *Phys. Rev. Lett.* **70** 1006
[30] Bruno P and Renard J-P 1989 *Appl. Phys.* A **49** 499